JOURNAL OF SPACECRAFT AND ROCKETS
Vol. 43, No. 4, July–August 2006

Engineering Notes

ENGINEERING NOTES are short manuscripts describing new developments or important results of a preliminary nature. These Notes should not exceed 2500 words (where a figure or table counts as 200 words). Following informal review by the Editors, they may be published within a few months of the date of receipt. Style requirements are the same as for regular contributions (see inside back cover).

New Calculation Method of Supersonic/Hypersonic Flow: Application to MESUR Capsule

Masatomi Nishio,* Keiji Manabe,† and Hiroaki Nakamura‡
Fukuyama University, Fukuyama 729-0292, Japan

DOI: 10.2514/1.17817

I. Introduction

In space development, it is vitally important to clarify the flowfield around supersonic/hypersonic vehicles [1–3]. Therefore, theoretical and experimental studies have been carried out by many researchers.

The studies on compressible flows using computational fluid dynamics are mainly carried out by means of the finite difference method (FDM) and the finite volume method. These methods have advantages of calculation times and memories when compared with the finite element method (FEM), and moreover the FDM has a high-resolution scheme such as the total variation diminishing method. Therefore, hardly any analyses using the FEM have been conducted.

To address these flaws, the authors and others have developed a new algorithm for compressible flow based on the FEM. The merit of this method is treatment of the pressure term in the Navier–Stokes equations. That is, the stress tensor including the pressure term is calculated as the nondifferential form in the weighted residual equation. By the use of this method for the analysis of compressible flows with shock waves, flowfields are calculated with more stable computation and less numerical error than that of conventional FEM analysis.

The validity of this method was confirmed by comparing the results with the shock wave and streamlines obtained by the electrical discharge method [4–7] for a hypersonic flow at Mach 10. In these comparisons, a Mars environmental survey (MESUR) capsule model was used.

II. Finite Element Method Formulation of Basic Equations

The Navier–Stokes equations of compressible flows can be written in the conservation form

$$\frac{\partial \boldsymbol{U}}{\partial t} + \left(\frac{\partial \boldsymbol{F}_i}{\partial x_i} + \underline{\frac{\boldsymbol{F}_2}{x_2}}\right) - \left(\frac{\partial \boldsymbol{G}_i}{\partial x_i} + \underline{\frac{\boldsymbol{G}'_2}{x_2}}\right) = 0 \tag{1}$$

where $\boldsymbol{U}$ is the vector of conservation variables and the particular form of the variables for Eq. (1) is presented in Eq. (2) and (3). Equation (1) represents the formulation for the two-dimensional and axisymmetric problems. The underlined terms are necessary when the problem is axisymmetric. In this paper, the summation convention is used for subscripts.

The particular form of the variables for Eq. (1) is

$$\boldsymbol{U} = \begin{bmatrix} \rho \\ \rho u_1 \\ \rho u_2 \\ \rho e \end{bmatrix}, \qquad \boldsymbol{F}_i = u_i \boldsymbol{U} = \begin{bmatrix} u_i \rho \\ u_i \rho u_1 \\ u_i \rho u_2 \\ u_i \rho e \end{bmatrix}$$
$$\boldsymbol{G}_i = \begin{bmatrix} 0 \\ \tau_{i1} - p\delta_{i1} \\ \tau_{i2} - p\delta_{i2} \\ u_m(\tau_{mi} - p\delta_{mi}) - q_i \end{bmatrix} \tag{2}$$

and

$$\boldsymbol{G}'_2 = \begin{bmatrix} 0 \\ \tau_{12} - p\delta_{12} \\ \tau_{22} - \tau_{\theta\theta} \\ u_m(\tau_{m2} - p\delta_{m2}) - q_2 \end{bmatrix} \tag{3}$$

where ρ is the fluid density, u_i represents the velocity components, e is the total energy per unit mass ($e = \varepsilon + u_i u_i/2$, ε is the internal energy), q_i represents the components of a heat flux vector, δ_{ij} is the Kronecker delta, and τ_{ij} is the component of the deviatoric stress tensor. In the case of the axisymmetric problem, Eq. (3) is considered. In Eq. (3), $\tau_{\theta\theta}$ is the deviatoric stress of circumference direction.

In the conventional FEM for the analysis of compressible flows, the pressure p is treated in the flux vector $\boldsymbol{F}_i$. However, as is shown in Eq. (2), p is included in the flux vector $\boldsymbol{G}_i$ in this study. The reason for this follows.

Boundary conditions on S_U and S_P are given as follows:

$$\boldsymbol{U} = \bar{\boldsymbol{U}}, \quad \text{on } S_U, \qquad \boldsymbol{G}_i n_i = \bar{\boldsymbol{P}}, \quad \text{on } S_P \tag{4}$$

where $\bar{\boldsymbol{U}}$ and $\bar{\boldsymbol{P}}$ are known quantities and n_i denotes the x and y components of the unit outward normal vector to S_p.

After multiplication of Eq. (1) by the weighting function w, integrating over the domain V, and applying the Gaussian divergence theorem, the following equation is obtained:

$$\int_V w \frac{\partial \boldsymbol{U}}{\partial t}\,\mathrm{d}V = -\int_V w \frac{\partial \boldsymbol{F}_i}{\partial x_i}\,\mathrm{d}V - \int_V \frac{\partial w}{\partial x_i}\boldsymbol{G}_i\,\mathrm{d}V + \int_{Sp} w\bar{\boldsymbol{P}}\,\mathrm{d}S - \underline{\int_V w\left(\frac{\boldsymbol{F}_2}{x_2} - \frac{\boldsymbol{G}'_2 - \boldsymbol{G}_2}{x_2}\right)\mathrm{d}V} \tag{5}$$

In Eq. (5), $\mathrm{d}V = 2\pi x_2\,\mathrm{d}x_i\,\mathrm{d}x_2$ if the problem is axisymmetric.

As shown in Eq. (5), $\boldsymbol{F}_i$ is the differential form and $\boldsymbol{G}_i$ is the nondifferential form. Thus, by applying partial integration, the rank of differentiation is reduced.

Received 21 October 2005; accepted for publication 24 January 2006.

*Professor, Department of Mechanical Engineering; m.nishio@fume.fukuyama-u.ac.jp. Senior Member AIAA.

†Associate Professor, Department of Mechanical Engineering. Member AIAA.

‡Research Associate.

When the momentum conservation law is applied to the second term on the right-hand side of Eq. (5), that is,

$$\left[\int_V \frac{\partial w}{\partial x_1}\boldsymbol{G}_1\,\mathrm{d}V + \int_V \frac{\partial w}{\partial x_2}\boldsymbol{G}_2\,\mathrm{d}V\right] \tag{6}$$

this term represents nodal point force, which is equivalent to internal stress according to the law of virtual work. Therefore, when the explicit method is applied by diagonalizing the matrix of the left-hand side of Eq. (5), the momentum conservation law of Eq. (5) directly shows the relation between the equivalent nodal force and the acceleration of the nodal points, that is,

$$\begin{aligned}&(\text{material derivative of nodal momentum})\\ &\quad = (\text{nodal internal force}) + (\text{nodal external force})\end{aligned} \tag{7}$$

Thus, it can be analyzed as a Newtonian equation of motion. By obtaining this relation, simultaneous equations do not need to be solved, and also, better stability and less error can be obtained in the calculations of the FEM.

To give numerical stability to the local flow direction, the streamline-upwind/Petrov–Galerkin method is introduced. In addition, $\nu\Delta\boldsymbol{U}$ ($\Delta\boldsymbol{U} = \partial^2\boldsymbol{U}/\partial x_i \partial x_i$) is incorporated as an artificial dissipation term. The symbol Δ is the Laplacian operator that is a second differential by the coordinates but is included in $\boldsymbol{G}_i$ as a first differential through partial integration, namely,

$$\boldsymbol{G}_i \leftarrow \boldsymbol{G}_i + \nu\frac{\partial \boldsymbol{U}}{\partial x_i} \tag{8}$$

In Eq. (8), ν denotes artificial viscosity.

III. Check of Calculated Flowfields Around Mars Environmental Survey Capsule

The flowfield around a MESUR capsule model traveling at a hypersonic speed of Mach 10 was calculated. In this case, the axisymmetric terms marked by the underline in Eq. (1) were considered, and the four-node quadrilateral element was used. The computational grid consisted of 194×100 nodal points, that is, the number of nodes was 19,695 and the number of elements was 19,400. The value of the calculation step was $\Delta t = 1.0 \times 10^{-8}$ s. To compare the result with the experimental one using a hypersonic gun tunnel, the simulation was carried out under these conditions: the Mach number was $M = 10$, the freestream density was $\rho = 4.5 \times 10^{-3}$ kg/m^3, the static pressure was $p = 70$ N/m^2, the static temperature was $T = 54$ K, and the freestream velocity was $V = 1500$ m/s. The flow was assumed to be the laminar flow ($Re = 9.75 \times 10^4$, reference length is 5.0×10^{-2} m). These values were the same as the experimental ones. For the boundary condition, the nonslip condition was applied for the surface of the model, and the surface was treated as the adiabatic wall.

Figure 1 shows the density contours around the capsule obtained by the present method (artificial viscosity ν is 0.1), and Fig. 2 shows the relation between streamline vs calculation step numbers. (In Fig. 2, Rf is the distance between the free shear layer at the location of $2Rb$ and the capsule axis.) From these results, it is found that the shock standoff distance Xs/Rb (where Xs is the shock standoff distance and Rb is the capsule radius) becomes stable at some 20,000 steps ($Xs/Rb = 0.216$) and the vortex region behind the capsule becomes larger with the calculation step numbers after that. In this simulation, flowfields around the capsule become stable at some 80,000 steps (Rs/Rb becomes 0.895, where Rs represents the distance between the separation point and the capsule axis). Figure 3

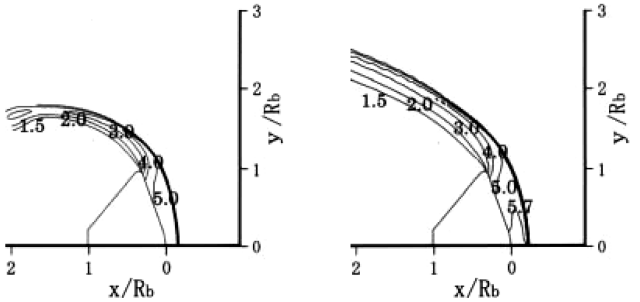

a) 10,1000 steps, *Xs/Rb*=0.149 c) 20,000 steps, *Xs/Rb*=0.216

b) 15,000 steps, *Xs/Rb*=0.213 d) 30,000 steps, *Xs/Rb*=0.216

Fig. 1 Calculated results of the density contours around the capsule obtained by the new calculation method at $M = 10$.

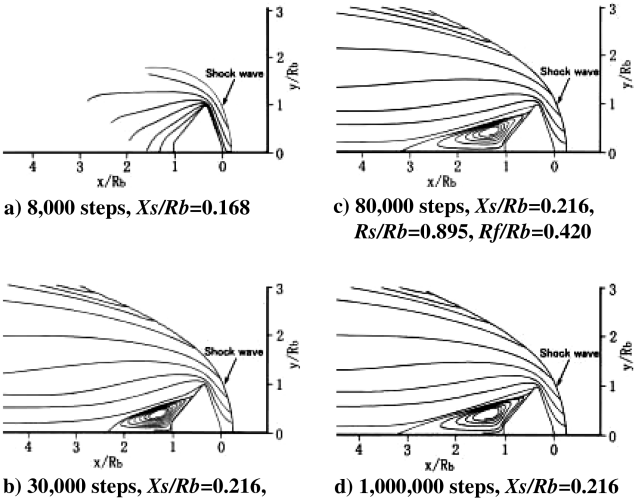

a) 8,000 steps, *Xs/Rb*=0.168 c) 80,000 steps, *Xs/Rb*=0.216, *Rs/Rb*=0.895, *Rf/Rb*=0.420

b) 30,000 steps, *Xs/Rb*=0.216, *Rs/Rb*=0.770, *Rf/Rb*=0.252 d) 1,000,000 steps, *Xs/Rb*=0.216 *Rs/Rb*=0.895, *Rf/Rb*=0.426

Fig. 2 Streamline vs calculation step numbers.

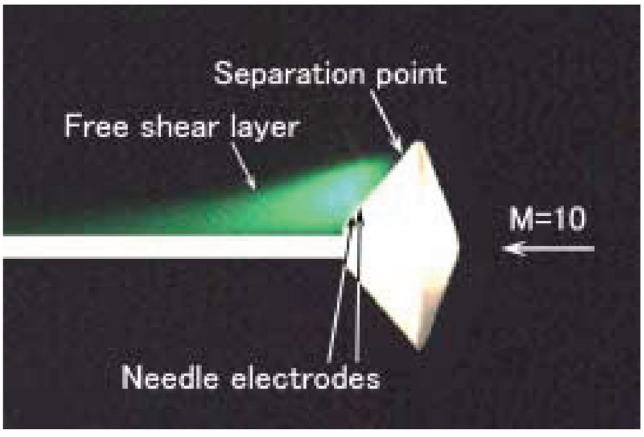

Fig. 3 Visualized result for the wake behind the capsule including the separation point and the free shear layer at $M = 10$.

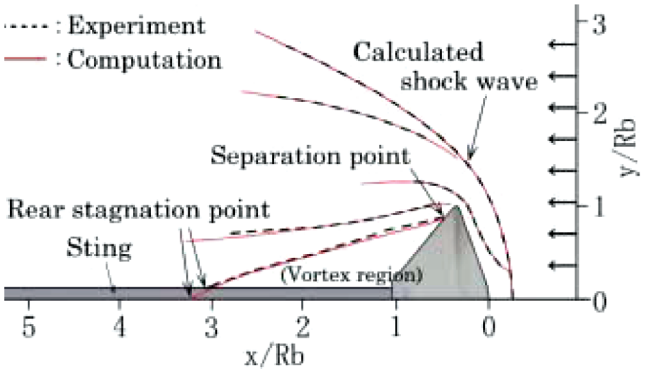

Fig. 4 Flowfields obtained by the new calculation method and the electrical discharge method [7] at $M = 10$.

shows the visualized result for the wake behind the capsule obtained by the electrical discharge method (Rs/Rb becomes 0.893 ± 0.003). Figure 4 shows the comparison of calculated results (the solid line) and visualized ones (the dotted line) [7] for flow structures around the capsule traveling at Mach 10. As described above, the value of shock standoff distance Xs/Rb becomes some 0.216, and the value of Rs/Rb becomes 0.893 to 0.895. Furthermore, streamlines around the capsule and the free shear layer almost perfectly agree. From these comparisons, it can be concluded that the calculated results are considerably accurate.

IV. Comparisons of Present and Conventional Methods

Comparisons of the computational results obtained by the new method and a conventional FEM were conducted.

First, as the value of artificial viscosity, $\nu = 0.1$ was used. In this case, the shock standoff distance Xs/Rb was nearly 0.633 [shown in Fig. 5a], showing that a large difference of the Xs/Rb value occurred compared with not only the present new method but also the experimental result (Xs/Rb was nearly 0.216).

Subsequently, to improve the shock standoff distance obtained by the conventional FEM, the value of artificial viscosity value was changed into 4 times ($\nu = 0.4$) that of the new method. This technique, that is, the treatment of artificial viscosity, is widely known to be convenient for stabilizing the numerical calculation. However, when the value of the artificial viscosity becomes larger, the computational result of the flowfield, such as the wake, would contain a greater error, as many researchers have already shown. Figure 5 shows calculated flowfields obtained by the conventional method using different artificial viscosity values. As we can see from the result in Fig. 5, when the value of artificial viscosity becomes larger, the shock standoff distance becomes more reasonable (in the case of the experimental result, $Xs/Rb = 0.216$, and in the case of the computational result, $Xs/Rb = 0.252$). However, the vortex region behind the capsule becomes very small, namely, the Rs/Rb value is 0.691, which is considerably smaller than the experimental values of $Rs/Rb = 0.893 \pm 0.003$ (shown in Fig. 3) and also compared with the new method value of $Rs/Rb = 0.895$.

From these results, it can be concluded that the new method is much more superior than the conventional method.

V. Conclusions

A new calculation method of flowfield around supersonic/hypersonic vehicles based on the FEM has been presented. The merit of this method was treatment of the pressure term in the Navier–Stokes equations. That is, the stress tensor including the pressure term was calculated as the nondifferential form in the weighted residual equation. By the use of this method for the analysis of compressible flows with shock waves, flowfields were calculated with more stable computation and less numerical error than that of conventional FEM analysis. The correctness of the present method

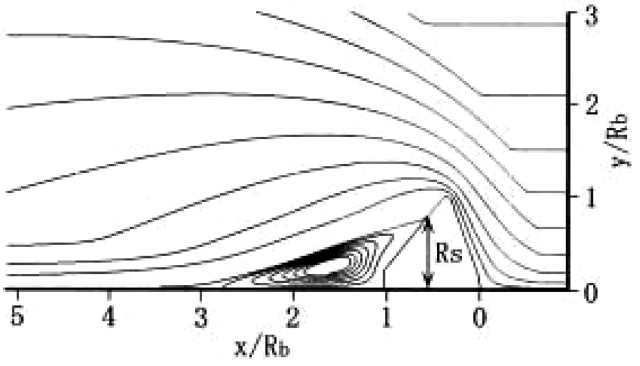

a) Artificial viscosity ν is 0.1, Xs/Rb=0.633, Rs/Rb=0.783, 100,000 steps

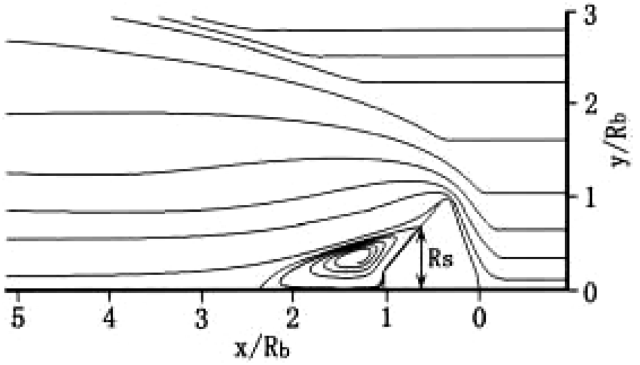

b) Artificial viscosity ν is 0.4, Xs/Rb=0.252, Rs/Rb=0.691, 100,000 steps

Fig. 5 Calculated result of the flowfield around the capsule obtained by the conventional method at $M = 10$.

was confirmed by comparing the shock shape, spatial streamlines, and the separation point. From these results, it could be concluded that the calculated results and visualized ones were in very good agreement. However, the conventional FEM results were very different from the experimental ones. The comparisons were carried out under the condition of a Mach 10 flow by using the MESUR capsule models.

References

[1] Olynick, D. R., Taylor, J. C., and Hassan, H. A., "Comparisons Between DSMC and the Navier-Stokes Equations for Reentry Flows," AIAA Paper 1993-2810, 1993.

[2] Kim, M. S., Loellbach, J. M., and Lee, K. D. "Effects of Gas Models on Hypersonic Base Flow Calculations," *Journal of Spacecraft and Rockets*, Vol. 31, No. 2, 1994, pp. 223–230.

[3] Seror, S., Zeitoun, D. E., Brazier, J.-PH., and Schall, E., "Asymptotic Defect Boundary Layer Theory Applied to Thermochemical Non-Equilibrium Hypersonic Flows," *Journal of Fluid Mechanics*, Vol. 339, May 1997, pp. 213–238.

[4] Nishio, M., "Method for Visualizing Streamline Around Hypersonic Vehicles by Using Electric Discharge," *AIAA Journal*, Vol. 30, No. 6, 1992, pp. 1662–1663.

[5] Nishio, M., "Methods for Visualizing Hypersonic Shock-Wave/Boundary-Layer Interaction Using Electric Discharge," *AIAA Journal*, Vol. 34, No. 7, 1996, pp. 1464–1467.

[6] Nishio, M., Sezaki, S., and Nakamura, H., "Measurements of Capsule Wake Stabilization Times in a Hypersonic Gun Tunnel," *AIAA Journal*, Vol. 42, No. 1, 2004, pp. 56–60.

[7] Nishio, M., Sezaki, S., and Nakamura, H., "Visualization of Flow Structure Around a Hypersonic Re-entry Capsule Using the Electrical Discharge Method," *Journal of Visualization*, Vol. 7, No. 2, 2004, pp. 151–158.

R. Cummings
Associate Editor